Aquatic Geochemistry
https://doi.org/10.1007/s10498-024-09429-4

ORIGINAL ARTICLE

Origin and Formation Mechanisms of Potassium- and Lithium-Rich Brines in the Triassic Strata of Northeastern Sichuan Basin, South China

Jiaai Zhong[1,4] · Yongjie Lin[2] · Fuming Wang[1] · Kelu Su[3] · Zhu Liu[1] · Debo Sheng[1] · Hongbin Li[1] · Bo Pang[1]

Received: 30 December 2023 / Accepted: 20 April 2024
© The Author(s), under exclusive licence to Springer Nature B.V. 2024

Abstract
The northeastern Sichuan Basin hosts deep brines with unusually high concentrations of potassium (K) and lithium (Li). This study examines deep brines abundant in K and Li in northeastern Sichuan Basin. Brine samples from Well ZK601 underwent comprehensive analysis for major elements, trace elements, and Sr isotopes. Lithium content in core samples correlated with regional brine reservoir features. Brine samples showed a salinity range of 354.6–363 g/L, with varying contents of Na^+ (101–106 g/L), K^+ (28.92–34.84 g/L), Cl^- (202.1–206 g/L), Br^- (2110–2980 mg/L), and Li^+ (169.5–204.5 mg/L). The $^{87}Sr/^{86}Sr$ ratio in brine was 0.708324. Li notably increased post-green bean rock deposition in 71 core samples. The ratios are as follows: $Br \times 10^3/Cl$ is 10.24, $K \times 10^3/Cl$ is 169.13, nNa/nCl is 0.74, and $SO_4 \times 10^3/Cl$ is 0.49. These brines likely originated from ancient seawater, evolving via rock interactions during burial, notably enriching K and Li through gypsum dehydration. Geochemical traits and Sr isotopes affirm ancient seawater origin, stressing continual water–rock interactions. The volcanic activity contributed significantly to lithium enrichment, consolidated during later burial stages. Brine reservoirs, mostly in formations like dolomite within the Jialingjiang Formation, associate closely with fractured zones. Structural traps define distribution, while fault systems govern enrichment. Accumulation mainly occurs in fractured zones, reflecting a mineralization model of seawater origins, metamorphism, filtration, and structural enrichment. In summary, our model outlines a transformation from seawater origins to structural controls enriching K and Li in deep brines in northeastern Sichuan Basin.

Keywords K- and Li-rich brines · Mineralization mechanisms · Structural enrichment processes · Sichuan Basin

✉ Yongjie Lin
linyongjie2014@163.com

[1] The 2, Geological Brigade of Sichuan, Chengdu, China

[2] MNR Key Laboratory of Saline Lake Resources and Environments, Institute of Mineral Resources, Chinese Academy of Geological Sciences, Beijing, China

[3] SINOPEC Exploration Company, Chengdu, China

[4] Sichuan University of Arts and Science, Dazhou, China

1 Introduction

The recent surges in demand for brine-based lithium (Li) and potassium (K) resources can be attributed to their crucial roles in a wide range of industries (Munk et al. 2016; Liu et al. 2023). Li is vital for electric vehicles and electronics, whereas K enhances agricultural productivity. Utilizing these resources is essential for sustainable energy shifts, better farming, and economic advancement (Wang et al. 2021). With rising worldwide demand, understanding their origins is critical for energy requirements, food stability, and tech progress.

The Xuanhan area, located in the northeastern part of the Sichuan Basin, holds significant importance as a major reservoir of oil and gas in China, notably hosting the Puguang gas field (Ma 2007). Within this gas field, the upper strata contain deeply seated, highly mineralized brines with total dissolved solids (TDS) reaching up to 330 g/L (Zhong et al. 2018a, b). These brines are found at depths ranging from approximately 3000 to 4000 m and contain exploitable levels of K, Li, bromine (Br), and boron (B), with notably high concentrations of K and Li (Zhong et al. 2018a, b). Song et al. (1988) have suggested that the concentrated brines in the northeastern Sichuan Basin exhibit characteristics resulting from a combination of marine and terrestrial sources. The enrichment of specific elements occurred during the late stage of salt formation when external brines and strata waters infiltrated salt basins, dissolving salt layers under evaporative conditions. Li et al. (1998) proposed that the brines from Well 25 in Sichuan are a mixture of sedimentary water and ancient leaching water influenced by the Indosinian movement. Additionally, Zhang et al. (2022) proposed that the genesis of potassium-rich brines in Northeast Sichuan primarily arises from seawater evaporation, concentration, and surface freshwater leaching mechanisms. These processes show a lesser influence from deep water–rock reactions, indicating a multifaceted genesis characterized by multiple stages. Despite decades of research on the potassium- and lithium-rich brines in the northeastern Sichuan Basin, a unified understanding of their genesis and enrichment patterns remains elusive.

In this study, we employed geochemical compositional analysis, strontium isotope analysis, and high-temperature and high-pressure experiments on the brine and its surrounding rocks. We aim to explore the origin and ore-forming model of the K- and Li-rich brines. This study holds significant importance in understanding the origin of K- and Li-rich brines, advancing our knowledge regarding the formation mechanisms of these enriched brines.

2 Geological Setting

The study area, situated in the northeastern Sichuan Basin (Fig. 1), lies within the core of the Sichuan foreland basin, part of the ancient Yangtze landmass at the northwest edge. During the Early to Middle Triassic, following the collision between the North China and South China plates in the Early to Late Permian period, and influenced by the Indosinian movement, the plateau edges underwent continuous uplift (Meng 2017; Zhang et al. 2019). This led to the formation of an elevated zone at the plateau margins. In the Early Triassic, the northwest of the ancient Yangtze landmass was notably higher in elevation compared to the southeast (Wen et al. 2023; Xu and Gong 2023). However, by the Middle Triassic, significant uplift occurred in the southeastern Jiangnan landmass, while the northwestern Longmenshan landmass subsided (Xu and Gong. 2023; Li et al. 2012). This

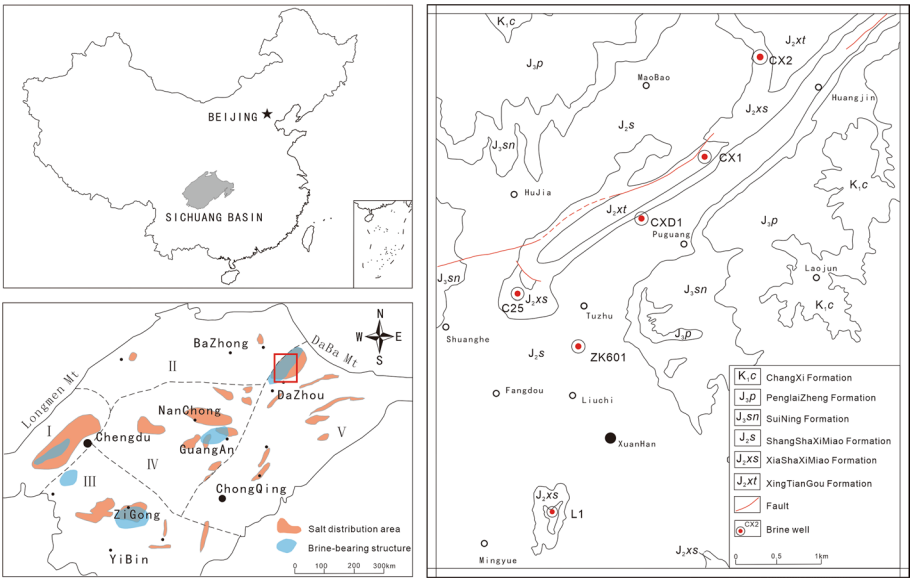

Fig. 1 Map of the study area and the position of salt-bearing structural (modified from Gong. 2016)

shift resulted in a topographical change, elevating the southeast and lowering the northwest. This movement forced seawater to retreat westward from the Yangtze region. Consequently, the Sichuan Basin, being farthest from seawater intrusion and replenishment, experienced minimal seawater dilution (Gong 2016). This condition favored salt deposition through evaporation, accumulating highly saline seawater. As a result, rock salt and even more saline salts, like potash–magnesium salts, were deposited (Fig. 2).

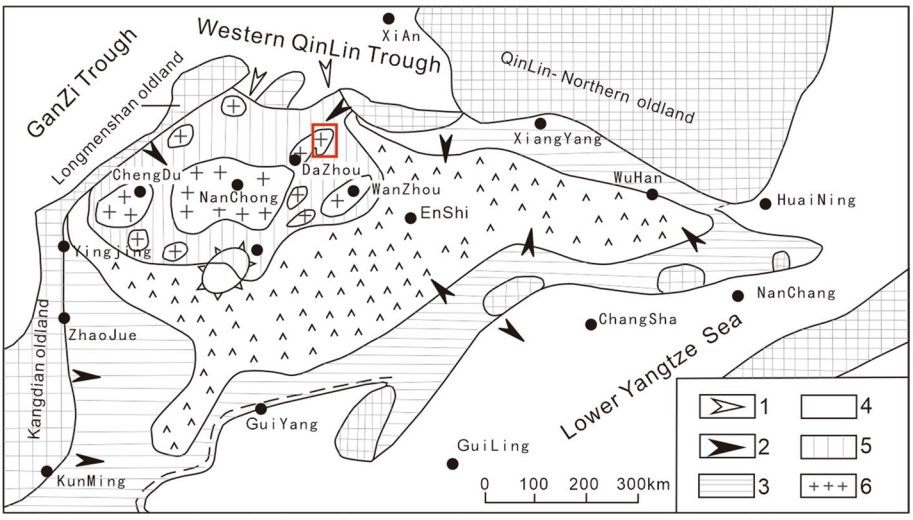

Fig. 2 Paleogeographical map of the upper Yangtze plateau during the Jialingjiang and Leikoupo period (Lin and Chen 2008)

During the Triassic in the Sichuan Basin, six salt-forming phases occurred across formations such as the Jialingjiang and Leikoupo Formations. These phases, totaling approximately 1000 m (m) in sedimentary thickness, comprised mainly alternating carbonate and evaporite rocks. Evaporite rocks constituted around 50% of the deposits, with rock salt making up 20% or more. In the Middle Triassic, a convergence of factors—shallow-water craton carbonate rocks, a warm arid climate, and declining sea levels—led to seawater concentration and increased salinity in the central region. This favored the deposition of potash salts (Chen et al. 2015). The northeastern part of Sichuan features principal salt-bearing strata from the Upper Lower Triassic Jialingjiang Formation to the Lower Middle Triassic Leikoupo Formation. These formations, spanning 100–400 m, predominantly consist of dolomitic limestone, occasionally interspersed with limestone, anhydrite, impure halite, and rock salt layers. These strata encompass dispersed brine layers within carbonate rocks and are demarcated by a gray–green muscovite claystone. This distinctive layer serves as a crucial regional marker bed (Wang et al. 2022) and, although widely distributed, may be absent in regions eroded due to uplift (Zhu and Wang 1986). The mineral composition of the "mung bean rock" in Well ZK601 comprises primarily potassium feldspar, mica, quartz, and clay minerals (Wang et al. 2022). In the eastern Sichuan area, this layer contains lithium adsorbed by clay minerals (Cheng et al. 1999), exhibiting significant lithium enrichment, with concentrations ranging from 127×10^{-6} to 663×10^{-6} (Wang et al. 2023; Sun et al. 2018; Ma et al. 2019).

3 Samples and Methods

3.1 Sample Collection

This study focused on the salt-bearing strata, brines, brine reservoirs, and related formations (such as carbonate, anhydrite, rock salt, and polyhalite) in the northeastern Sichuan Basin. Three samples were collected for chemical analysis of the brines, and one sample was allocated for Sr isotope analysis. Additionally, a systematic collection of 71 core samples was sampled based on depth and lithology.

3.2 Chemical Composition Analysis

The determination of major and trace elements in brines was conducted at the Chinese Academy of Geological Sciences. The concentrations of Li^+, Na^+, K^+, Rb^+, Cs^+, Mg^{2+}, Ca2+, and Sr^{2+} in the brines were measured using atomic absorption spectrophotometry. Cl^-, HCO_3^-, OH^-, CO_3^{2-}, and B_2O_3 were analyzed using volumetric methods. Br was tested using the phenol red colorimetric method. SO_4^{2-} content was determined through weight methods, with a systematic error of 1.6%.

3.3 Strontium Isotope Analysis

The measurement of strontium isotope composition in the brines was performed using the TIMSVG-354 isotope mass spectrometer at the Isotope Solid Spectrometry Laboratory of the State Key Laboratory for Mineral Deposits Research, Nanjing University. The NBS-987 standard yielded an average $^{87}Sr/^{86}Sr$ value of 0.710250 ($n=8$), normalized to $^{87}Sr/^{86}Sr=0.1194$. The error for each sample analysis was less than $\pm0.05\%$.

3.4 High-Temperature and High-Pressure Simulation Experiments

High-temperature and high-pressure simulation experiments were conducted at the High-Temperature and High-Pressure Simulation Analysis Laboratory, Lanzhou Center for Oil and Gas Resources, Institute of Geology and Geophysics, Chinese Academy of Sciences. The experiments utilized the WYMN-3 high-temperature and high-pressure simulation apparatus. A high-pressure vessel was employed to simulate geological pressures, gradually heating the samples to predetermined temperatures within 2 h and maintaining a constant temperature. Upon reaching the set temperature, the instrument automatically depressurized via drainage based on preset pressure thresholds. Liquid and solid samples generated during the constant temperature phase were collected for analysis. Experiment temperatures and pressures were set based on regional geothermal gradients, lithostatic pressure coefficients, and the burial history of the strata.

Utilizing reflectance data from the previously measured Puguang Gas Field, simulations indicated a Mesozoic critical geological period with a paleogeothermal gradient of 3.0 °C/100 m in the northeastern Sichuan region (Zhu et al. 2017). Thus, a paleogeothermal gradient of 3.0 °C/100 m and a paleosurface temperature of 15 °C were applied to design specific temperature points for the simulations. Overlying strata in the research area comprise Upper Jurassic and Triassic continental strata predominantly composed of clastic rocks such as sandstone and shale, with an average density of 2.25 g/cm^3. Lithostatic pressure coefficients in northeastern Sichuan generally range between 1.06 and 1.49, with coefficients for the Upper Triassic Leikoupo Formation ranging from 1.06 to 1.30 and the Jialingjiang Formation ranging from 1.10 to 1.37. For this experiment, a pressure coefficient of 1.25 was utilized to design specific lithostatic pressures based on simulated depths. Based on the burial history of the Upper Triassic strata in the Puguang 2 Well area in northeastern Sichuan, the maximum burial depth of the Jialingjiang Formation is approximately 6700 m. According to the paleogeothermal gradient and paleosurface temperature, the maximum burial depth of the Jialingjiang Formation in the study area corresponds to a stratal temperature of 216 °C. Thus, experiments were conducted at simulated temperatures ranging from 105 to 220 °C, designed for burial depths of 3500 m, 5000 m, and 6700 m in three sets of simulations. Table 1 summarizes the simulated temperatures and pressures based on the aforementioned key parameters.

4 Results

4.1 Li Contents in Marine Sediments

A total of 71 samples of marine sediments were analyzed for Li content, with concentrations ranging from 1.1 to 375.25 μg/g (Fig. 3), and an average concentration of 65.39 μg/g.

Table 1 Parameters for the first set of simulation experiments

Simulated depth/m	Temperature/°C	Pressure/Mpa	Simulation time/h
3500	120	78.75	72
5000	165	112.5	72
6700	220	150.75	72

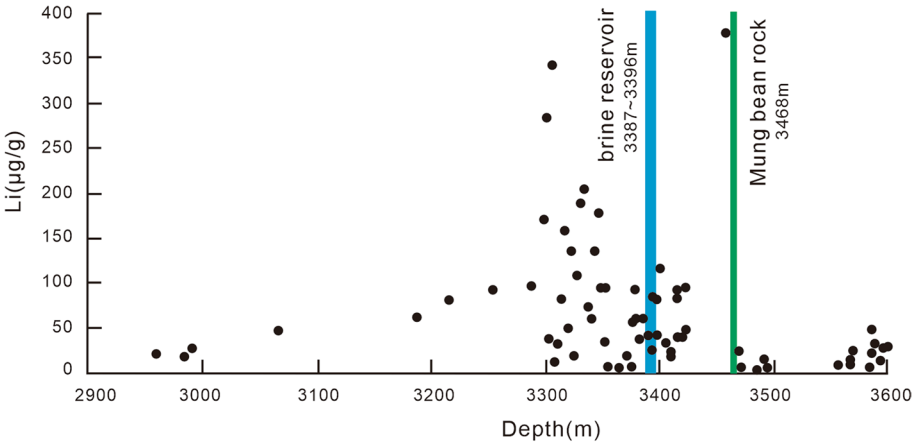

Fig. 3 The Li content as a function of depth in marine sediments

Below the Mung Bean Rock (MBR) at depths exceeding 3468 m, sediment Li concentrations ranged from 1.92 to 47.08 μg/g, averaging 14.44 μg/g. Post-deposition of the MBR, within the depth range of 3200–3468 m, Li concentrations in sediments varied from 1.65 to 375.25 μg/g, with an average of 86.25 μg/g. However, between depths of 2960 and 3200 m, there was a notable decline in sediment Li content, ranging from 16.92 to 94.68 μg/g, and averaging 34.21 μg/g.

4.2 Chemical Compositions of Brine

Three samples of brine were collected from different time intervals during the pumping test of Well ZK601, exhibiting salinity levels ranging from 354.6 to 363 g/L (Table 2). The Na^+ content varied between 101 and 106 g/L, K^+ content between 28.92 and 34.84 g/L, Mg^{2+} content between 887 and 1077 mg/L, Ca^{2+} content between 9520 and 11,260 mg/L, Cl^- content between 202.1 and 206 g/L, SO_4^{2-} content between 1032 and 2294 mg/L, and HCO_3^- content between 671.2 and 1337.0 mg/L. The hydrochemical classification is calcium chloride type. In addition, Li^+ content ranged between 169.5 and 204.5 mg/L, Br^- content between 2110 and 2980 mg/L, Rb^+ content between 36.8 and 53 mg/L, and I^-content between 31.37 and 36.3 mg/L. The pH value of brine ranged between 7.5 and 7.7. One sample of brine, analyzed for Sr isotopes, exhibited an $^{87}Sr/^{86}Sr$ ratio of 0.708324 in the ZK601 well's brine.

Table 2 Analysis results of brine samples

Sample no.	Li^+ mg/L	K^+ mg/L	Na^+ mg/L	Mg^{2+} mg/L	Cl^- mg/L	HCO_3^- mg/L	Br^- mg/L	B mg/L	Rb mg/L
1	169.5	28,920	106,000	887	202,100	1337	2510	1790	36.8
2	204.5	34,800	101,000	1077	206,000	666.8	2980	2173	53
3	201.5	34,840	102,400	1031	206,000	671.2	2110	2198	51

4.3 High-Temperature and High-Pressure Simulation Experiment Results

XRD revealed that under the temperature and pressure conditions of the target strata in the study area, gypsum ($CaSO_4 \cdot 2H_2O$) dehydrated at 165 °C, producing hemihydrate gypsum ($CaSO_4 \cdot 1/2H_2O$), and completely transformed into anhydrite ($CaSO_4$) at 220 °C. The process involved is: $CaSO_4 \cdot 2H_2O \rightarrow CaSO_4 \cdot 1/2H_2O + 3/2\ H_2O$ (solvent) $\rightarrow CaSO_4 + 2H_2O$ (solvent) (Fig. 4). The hundreds of meters thick anhydrite rocks of the Jialingjiang Formation and Leikoupo Formation in this region (Zhong et al. 2020) likely originate from the dehydration of primary gypsum, a process that releases a substantial amount of liquid water.

5 Discussion

5.1 Origin of Deep Brine in the Northeastern Sichuan Basin

Deep brines are stored within specific rock formations made of carbonate and evaporite rocks, closely linked to the process of seawater concentration through evaporation (Zheng et al. 2012a, b). Comparing the chemical composition of remaining brine from seawater evaporation with that found underground helps understand where these brines come from. Carpenter (1978) described five main stages of mineral formation when seawater evaporates, including gypsum, halite, mirabilite, potassium salts, and bischofite. In further experiments with South China seawater at 25 °C, seven stages of salt formation during seawater evaporation, which involved calcite, gypsum, halite, mirabilite, potassium salts, carnallite, and bischofite (Li and Han 1995). The salinity levels of the ZK601 well brine match those seen during the mirabilite stage of typical brine evaporation. However, when comparing the consistent components with what's seen during mirabilite sedimentation in seawater, the brine shows differences. It has lower levels of Mg^{2+} and SO_4^{2-} but higher amounts of K^+ and Ca^{2+}. This suggests that there are other factors influencing how this brine has evolved. The $^{87}Sr/^{86}Sr$ ratio in the ZK601 well brine, at 0.708324 (Fig. 5), falls within the range of $^{87}Sr/^{86}Sr$ isotope values (ranging from 0.70816 to 0.70837) found in polyhalite, halite, anhydrite, and dolomite from the same Jialingjiang Formation in the well. This

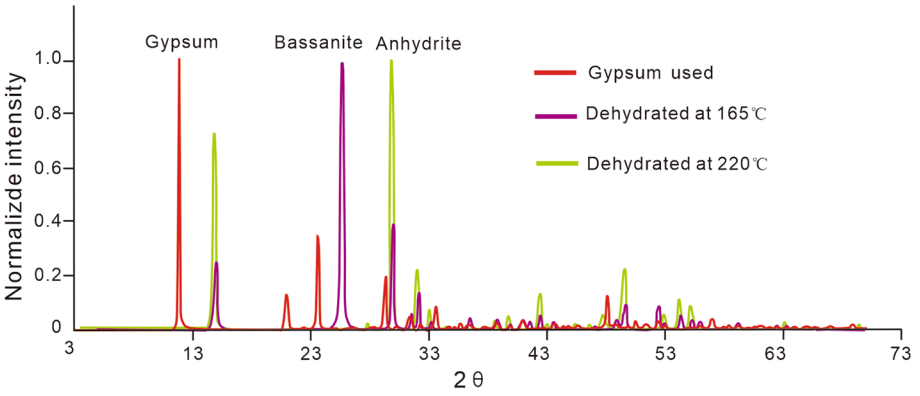

Fig. 4 XRD patterns of simulated experimental products

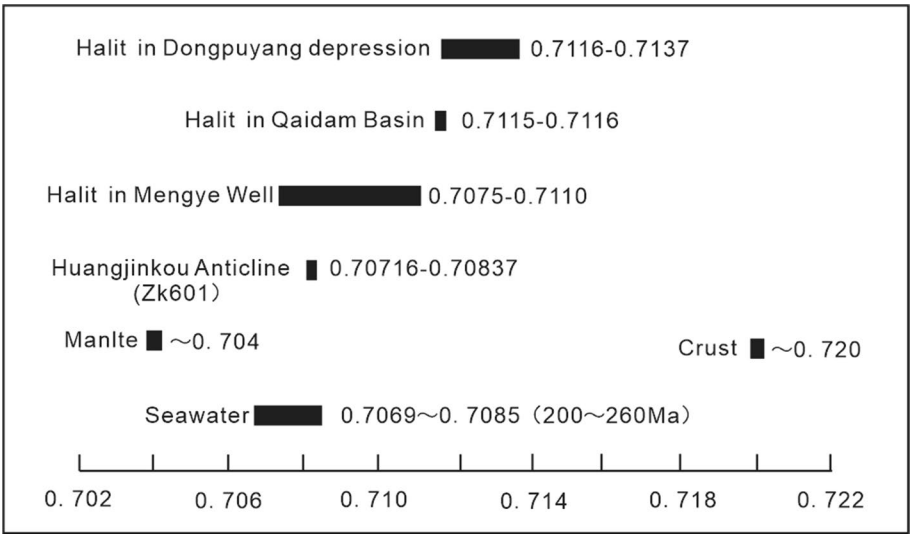

Fig. 5 Strontium isotope ratios from different sources (Crust and mantle data from Kelts (1987); oceanic data from Burke et al. (1982); Hess et al. (1986); salt rocks from Qaidam Basin and Dongpu depression represent Terrigenous salt samples from Tan et al. (2010); Shi et al. (2005); Mengye Well salt rock data represent salt samples primarily supplied by seawater with mixed terrigenous water, from Zheng et al. (2012a, b))

range aligns with what's expected from Triassic seawater strontium isotope data (Zhong et al. 2020). It confirms that the brine has origins linked to ancient marine sources.

5.2 Ratio of Brine Ion Coefficients

The brine contains higher concentrations of trace elements such as B_2O_3, I^-, Sr^{2+}, Li^+, Rb^+, and others compared to seawater. These concentrations are between 2.04 and 79.18 times higher than the maximum concentrations observed in normal seawater evaporation (Table 3), indicating a significantly elevated characteristic. Different groundwater sources or conditions lead to noticeable variations in the ratios of certain ion coefficients. These ratios are often used to infer the origin or genesis of underground water quality. During seawater evaporation and concentration, Br remains mostly in solution and does not

Table 3 Trace element characteristics of Well ZK601 (mg/L)

Sample	B^{3+}	I^-	Sr^+	Li^+	Rb^+
ZK601	2198.00	31.67	620.50	201.50	51.00
Chuang 25	1440.00	38.00	597.00	323.00	32.20
Highest content in seawater evaporation series	1077.83	0.40	59.85	45.24	7.00
ZK601/maximum content in seawater	2.04	79.18	10.37	4.45	7.29

participate significantly in reactions to form solid minerals, resulting in its concentration linearly increasing with seawater concentration. The $Br \times 10^3/Cl$ ratio in the ZK601 borehole brine is 10.24, corresponding to the initial mirabilite deposition stage during seawater evaporation. The $K \times 10^3/Cl$ ratio serves as an indicator of brine concentration, with a coefficient of 169.13 indicating higher concentration compared to potassium salts sedimentation during seawater evaporation stages. The nNa/nCl ratio reflects sodium salts enrichment in the brine, with a ratio of 0.74 for this brine, indicating a confined environment. The $SO_4^{2-} \times 10^3/Cl$ desulfurization coefficient reflects the enclosed nature of the brine formation environment. A smaller desulfurization coefficient signifies better closure conditions and stronger reducing conditions (Zhou et al. 2015). The ZK601 well brine has a $SO_4^{2-} \times 103/Cl$ ratio of 0.49, indicating a confined environment rich in organic matter and intense reducing conditions. From the brine salinity, concentrations of major and trace elements, nNa/nCl, $K \times 10^3/Cl$, $Br \times 10^3/Cl$, and $SO_4 \times 10^3/Cl$ ratios, it is evident that the brine undergoes water–rock interaction during long-term burial and confinement, rather than simply forming through evaporation and concentration of seawater.

The data for Well Chuan 25 are sourced from the publication by Wang et al. (1987)

5.3 Sources of K and Li in Deep Brine

R-type cluster analysis was performed on brine samples from Huangjinkou Anticline's ZK601 well, Chuan25 well, Bei2 well, Hengcheng1 well, and Dawan3 well using salinity and major ion concentrations as variables (Fig. 6). Salinity exhibits a correlation coefficient of 0.9784 with Cl^-, suggesting potential addition of chloride salts. B_2O_3 demonstrates a correlation coefficient of 0.9456 with Li^+ (Fig. 7), potentially indicating its association with the Green Bean Formation. Additionally, Na + shows a high correlation with Br^-, and Mg^{2+} exhibits a high correlation with SO_4^{2-}.

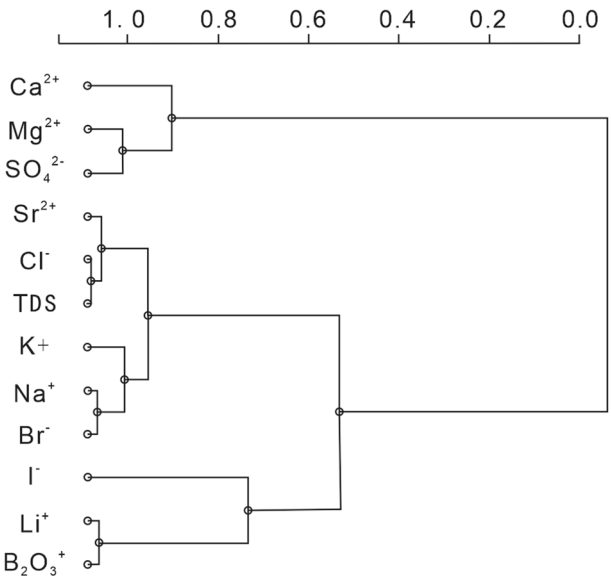

Fig. 6 Hierarchical clustering analysis of constant elemental contents in brine

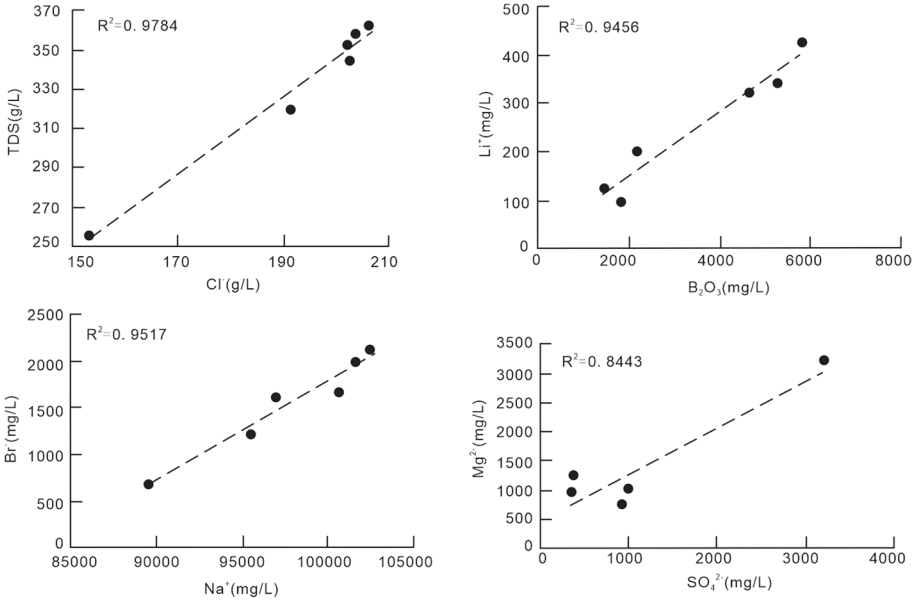

Fig. 7 Correlation analysis of constant elemental contents in brine

The brine layer in the ZK601 well coincides with polyhalite, anhydrite, and dolomite, with the present polyhalite layer reaching a total thickness of 34 m (Zhong et al. 2018a, b). High-temperature, high-pressure experiments indicate that gypsum remains as hemihydrate gypsum at depths up to 5000 m, converting entirely into anhydrite at 6700 m, signifying a continuous dehydration process for gypsum. The theoretically released crystalline water from gypsum dehydration equals 48.6% of the gypsum volume (Lin et al. 2005). The previous studies suggest that polyhalite can dissolve under different solvent conditions (Wang et al. 2011; An 2008). Considering the thickness of the polyhalite layer in the study area ranging from 1.3 to 84.7 m (Zhong et al. 2020), we propose that during the later burial stages, the substantial water slowly released from gypsum conversion dissolved parts of the solid potassium salt layers under high-temperature and high-pressure conditions. This process played a crucial role in the increase in potassium content in the brine.

During the seawater evaporation and concentration process, Li^+ remains solely in the liquid-phase brine. However, the Li^+ content in ZK601 is 20.45 times higher than that in the mirabilite stage brine. This suggests that the source of Li^+ cannot solely originate from simple leaching of gypsum dehydration from normal sedimentary carbonate rocks, anhydrite, or salt rocks. Looking at the variation in lithium content in marine sediments, below the 'Mung Bean Rock' layer, the Li content in sediments is relatively low. In the eastern Sichuan area, lithium content in sedimentary 'Mung Bean Rock' can reach 663×10^{-6} (Sun et al. 2018). After the deposition of 'Mung Bean Rock', the Li content in upper-layer sediments significantly increases. However, the lithium content in higher strata of marine sediments returns to levels before 'Mung Bean Rock' deposition, indicating that for a certain period after 'Mung Bean Rock' deposition, it continued to provide a material source for lithium in subsequent marine sediments. During the burial and compaction process of marine sediments, it further dissolved, serving as a source of lithium for the sealed brine. Although 'Mung Bean Rock' is widely distributed in the northeastern Sichuan area, among

numerous oil and gas wells and potassium exploration wells in the research area, residual 'Mung Bean Rock' has only been found in ZK601 well (Wang et al. 2022), indicating 'Mung Bean Rock' dissolution in the region.

5.4 Tectonic Controls on Brine Enrichment in the Sichuan Basin

A comparison of brine reservoirs from wells drilled in the 1970s and 1980s, including Chuan25, Bei2, Hengcheng1 (constructed by Hengcheng Corporation), ZK601 (constructed by the 405 Geological Team of the Provincial Bureau of Geology), and Dawan3 (constructed by PetroChina Puguang Gas Field), reveals that all brine reservoirs are situated in the upper part of the Jialingjiang Formation (restratified for comparative purposes according to the Puguang Gas Field stratigraphic criteria) Fig. 8. The lithology of the brine layer in ZK601 primarily consists of dolomite, dolomitic limestone, and dolomitic limestone, mostly located in fractured and broken zones (Fig. 9). During drilling, phenomena such as welling, leaking, and venting occurred, leading to an increase in Cl^-. The cores displayed porosity, fractures, fragmented structures, and structural breccias, exhibiting fault characteristics. Grainy native sulfur was observed on fault surfaces, while the cores often displayed phenomena such as halite immersion, retrogression, and salt frosting. The average porosity of the Leikoupo Formation reservoir section in ZK601 well is 2.57%, and permeability values are all less than 0.1 md. In contrast, the Jialingjiang Formation reservoirs show an average porosity of 3.97% and an average permeability of 0.027 md, indicating a low-porosity and low-permeability fractured-pore-type reservoir (Zhang et al. 2022).

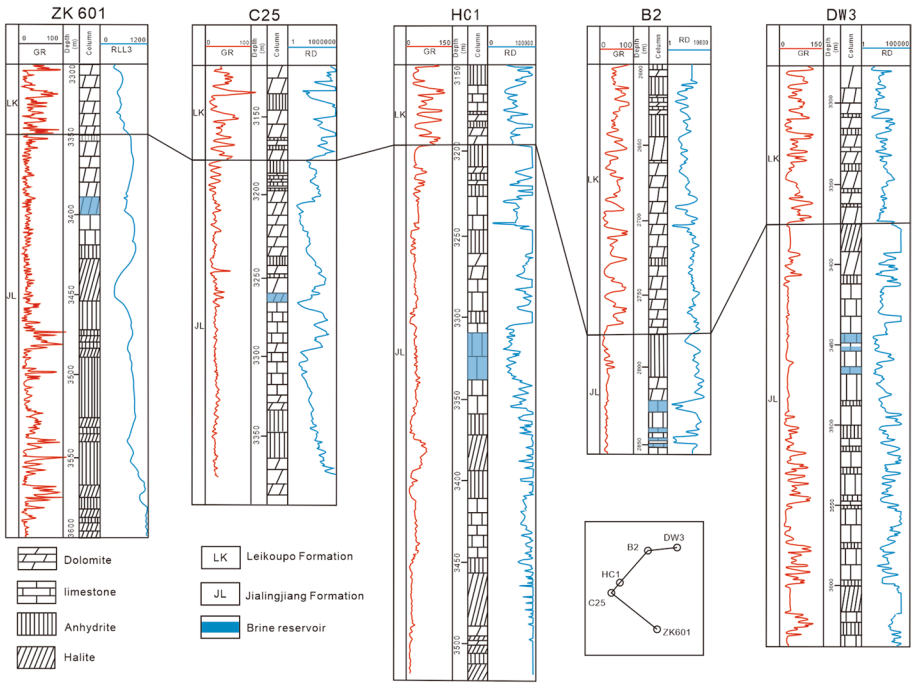

Fig. 8 Comparative diagram of brine reservoirs in the Huangjinkou Anticline

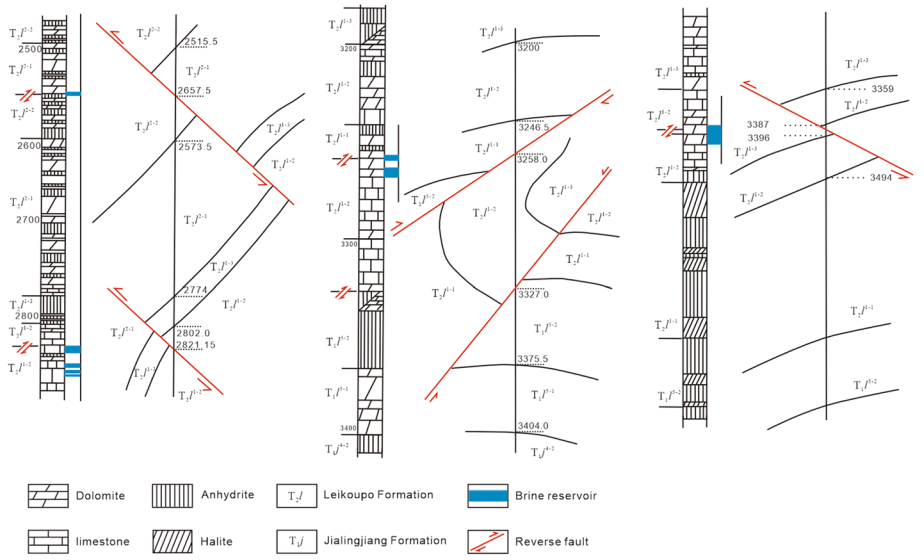

Fig. 9 Comparison of brine outcrop locations and structures in wells north 2, Chuan 25, and ZK601 in the Huangjinkou Anticline

The previous studies on Sichuan Basin brine reservoirs, irrespective of the degree of pore development, generally exhibit poor porosity and permeability overall, with only localized areas showing relatively good porosity, demonstrating anisotropic karst fracture reservoir characteristics (Lin and Zhao 1999). This feature does not favor the migration and accumulation of high salinity brines from deep layers. Therefore, the development of fractures becomes crucial (Yan 2012). Fractures not only promote the development of secondary pores but also expand the brine storage space, significantly improving migration conditions. The enrichment of brine water often correlates with regions of relatively concentrated tectonic stress and developed fault-fracture systems (Lin and Zhao 1999; Yan 2012). Considering the tectonic movement history in this region, after the marine sedimentary strata of the Leikoupo Formation ended, the northeastern Sichuan region experienced the Indosinian movement, Yanshan movement, and Himalayan movement. The compression during the Yanshan movement led to the formation of several low-amplitude structural belts and sinuous folds oriented northeast. During the early stage of the Himalayan movement, the main stress direction came from the northwest, creating a series of northeast-oriented asymmetric folds and fractures. In the later stage, influenced by the continued subduction of the Indian plate toward the Eurasian plate and intense uplift of the Dabashan mountain range, the primary stress direction in northeastern Sichuan evolved into northeast–southwest, causing the early northeast-oriented structures to be superimposed and modified by the later northwest-oriented structures, forming complex overlapping deformations (Tang et al. 2008).

Due to the impact of multiple phases of tectonic movements, tensional fractures often appear at the tops and turning points of anticlines, alongside the development of thrust faults. The development of faults often forms a primary fracture system in fault zones, connecting the same or different brine reservoir layers, creating significant interconnected spaces conducive to large-scale brine enrichment and accumulation.

Consequently, the presence of brine is controlled by both structural and fault controls, where structural traps define the distribution range of brine, and fault structures determine the extent of brine enrichment. Transitional complex regions, due to the transformation and overlapping of earlier structures by later structures, intensified folding, and developed fractures, became favorable zones for brine enrichment.

5.5 Mineralization Model

Seawater evaporation led to the formation of solid potassium salt polyhalite and brine, coinciding with volcanic eruptions that formed the MBR, a source of Li in the basin's brine. Subsequent burial and compaction processes underwent intense hydrothermal alteration and continuous gypsum dehydration. Water–rock interactions between dissolved potassium salts and the Green Bean Formation acted as sources for K and Li in the brine (Fig. 10). Over various tectonic events, deeply buried brines in the basin gradually converged toward fractured zones at the tops and turning points of anticlines. During brine migration, it selectively dissolved salt minerals and the MBR within the strata, resulting in deep-seated brine deposits rich in K and Li. Therefore, the mineralization model for the northeastern Sichuan Basin derives from seawater, undergoes alteration at depth, experiences dissolution effects from nearby sources, and enriches due to structural controls.

(I. Seawater evaporates, concentrating to form potassium salts, while mung bean rock dissolves in water, precipitating lithium. II. Polyhalite forms during the intrusion of seawater into ancient brine repeatedly. III. Detrital polyhalite potassium deposits are formed during burial and compaction. Potassium leaches out due to intergranular water and water from gypsum dehydration. IV. Brine migrates toward traps controlled by structures and lithology during the Yanshan–Himalayan period.)

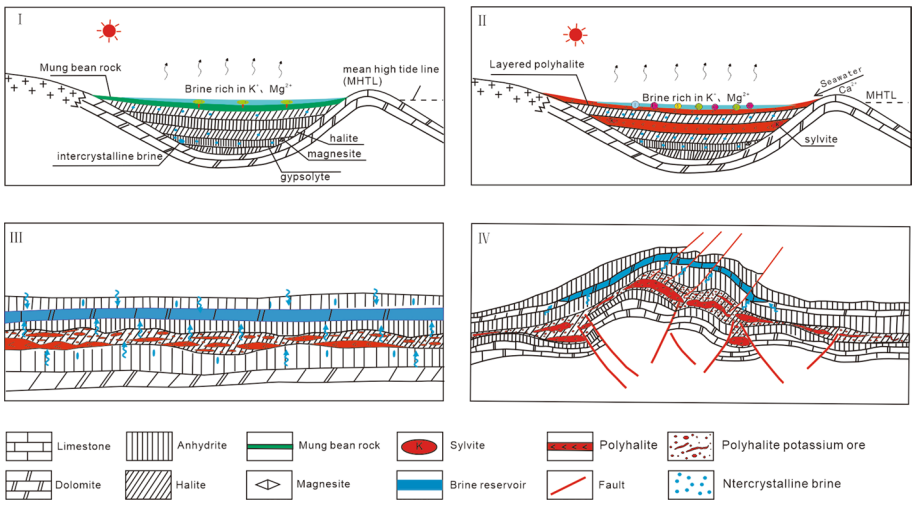

Fig. 10 Mineralization model of K- and Li-rich brine in Sichuan Basin

6 Conclusion

The geochemical signatures of trace elements and Sr isotopic ratios in the deep brines firmly establish their roots in ancient seawater within northeastern Sichuan. However, their formation was not a straightforward result of mere evaporation and concentration. Instead, it involved sustained water–rock interactions during subsequent deep burial and sealing processes, indicating a complex genesis. The concentration of brine witnessed contributions from the MBR, a product of contemporaneous volcanic eruptions, serving as the lithium source in the basin. Additionally, stages of burial saw continuous dissolution of solid potassium salts and gypsum dehydration, further enriching the brine with K and lithium Li. Brines predominantly occupy the upper part of the Jialingjiang Formation, situated amidst dolomite, dolomitic limestone, and fractured zones. Their presence is intricately linked to structural configurations and fault systems. Structural traps define the distribution of brine, while fault structures play a pivotal role in its enrichment. Therefore, the mineralization model for northeastern Sichuan encapsulates a narrative of seawater origin, transformation at depth, localized dissolution effects, and enrichment governed by structural controls. This study offers insights into the intricate processes shaping brine reservoirs, shedding light on their formation and enrichment mechanisms within the geological framework of northeastern Sichuan.

Acknowledgements This research was funded by the project "Core Technology Research and Application of Deep Potassium-Lithium Resource Exploration and Development" (Grant No.: KJCX-2022-014) and "A Potash Exploration Method for Sichuan Basin Based on Remote Sensing and Radioactive Energy Spectroscopy: Taking the Potash Salt of Polyhalite in the Huaying Mountain Area of Northeast Sichuan as an Example" (Grant No.: SCDZ-KJXM202403).

Authors' Contribution Jiaai Zhong helped in conceptualization, methodology, and writing—original draft. Yongjie Lin contributed to writing—review & editing. Fuming Wang contributed to writing—review & editing. Kelu Su contributed to writing—review & editing. Zhu Liu contributed to writing—review & editing. Debo Sheng contributed to writing—review & editing. Hongbin Liu contributed to writing—review & editing. Bo Pang contributed to writing—review & editing.

Data Availability No datasets were generated or analyzed during the current study.

Declarations

Conflict of interest The authors declare no competing interests.

References

An LY, Yang ZJ, Liu N, Yin HA, Tang ML (2008) Modeling of leaching process of polyhalite in laboratory. IM & P 37(10):24–27 (in Chinese)

Burke WH, Denison RE, Hetherington EA, Koepnick RB, Nelson HF, Otto JB (1982) Variation of seawater 87Sr/86Sr throughout Phanerozoic time. Geology 10(10):516–519

Carpenter AB (1978) Origin and chemical evolution of brines in sedimentary basins. In: SPE Annual Fall Technical Conference and Exhibition, OnePetro

Chen AQ, Wang LC, Ji GJ, Cao K, Xu SL, Tang WB (2015) Evaporatic environment and the concentration model of potash in the Early-Middle Triassic, northeastern Sichuan basin. Acta Petrol Sin 31(9):2757–2769 (**in Chinese**)

Cheng Z, Shen MD, Zhao JS, Tang HM (1999) New analysis on the composition of mung bean rock. J Southwest Pet Inst 21(1):39–42 (**in Chinese**)

Gong DX (2016) The Triassic salt-forming enviroment, potash-forming conditions and genetic mechanism in Sichuan basin. Ph. D. Dissertation, Chengdu University of Technology, Chengdu, pp 1–152 (in Chinese)

Hess J, Bender ML, Schilling JG (1986) Evolution of the ratio of strontium-87 to strontium-86 in seawater from Cretaceous to present. Science 231(4741):979–984

Kelts K (1987) Lacaustrine basin analysis and correlation by strontium isotope stratigraphy. Abstract of 13rd International Sedimentary

Li YW, Han WT (1995) Experimental study of 25℃ isothermal evaporation of sea water from the south China sea. Sci Geol Sin 30(3):233–239 (**in Chinese**)

Li YW, Cai KQ, Han WT (1998) Origin of potassium-riched brine and the metamorphism of Triassic evaporites in Sichuan basin. Geoscience 12(2):222–228 (**in Chinese**)

Li L, Tang XC, Zou C, Ding X, Yang G, Ying DL (2012) Origin of the Leikoupo Formation gypsum-salt and migration evolution of the gypsum-salt pot in the Sichuan basin, and their structural significance. Acta Geol Sin 86(2):316–324 (**in Chinese**)

Lin YT (2005) On the formation of groundwater in the Lower-Middle Trias series (T1j–T2l) of Sichuan basin. J Salt Lake Res 13(1):1–6 (**in Chinese**)

Lin YT, Chen ZL (2008) Discussion on the evaporite generating modes, saltforming mechanism and potassium-hunting prospect of Lower-Middle Triassic in Sichuan basin. J Salt Lake Res 16(3):1–10 (**in Chinese**)

Lin YT, Zhao ZJ (1999) A study of Triassic brine reservoir and brine accumulation regularities in the Sichuan basin. Acta Geol Sichuan 19(2):59–64 (**in Chinese**)

Liu C, Lowenstein TK, Wang A, Wang AJ, Zheng CM, Yu JG (2023) Brine: genesis and sustainable resource recovery worldwide. Annu Rev Environ Resour 48:371–394

Ma YS (2007) Generation mechanismof Puguang gas fieldin Sichuan Basin. Acta Pet Sin 28(2):9–14 (**in Chinese**)

Ma SC, Wang DH, Sun Y, Li C, Zhong HR (2019) Geochronology and geochemical characteristics of Lower-Middle Triassic clay rock and their significances for prospecting clay-type lithium deposit. Earth Sci 44(02):427–440 (**in Chinese**)

Meng QR (2017) Origin of the Qinling mountains (in Chinese). Sci Sin Terrae 47:412–420. https://doi.org/10.1360/N072016-00422

Munk LA, Hynek SA, Bradley DC, Boutt D, Labay K, Jochens H (2016) Lithium brines: A global perspective. Rare Earth and Critical Elements in Ore Deposits, Philip L. Verplanck, Murray W. Hitzman

Shi ZS, Chen KY, Sheng HE (2005) Strontium, sulfur and oxygen isotopic composition and significance of paleoenvironment of paleogene of dongpu depression. Earth Sci-J China Univ Geosci 30(4):430–436 (**in Chinese**)

Song HB, Song ZP, Xiao ZQ (1988) Stable isotope geochemistery of potash-rich brine in No.25 well of Xuanhan area in northeastern Sichuan and its potash-prospecting application. Bull Inst Miner Depos Chin Acad Geol Sci 1:51–67 (**in Chinese**)

Sun Y, Wang DH, Gao Y, Hang JY, Ma SC, Fan XT, Gu WS, Zhang HL (2018) Geochemical characteristics of lithium-rich mung bean rocks in Tongliang County, Chongqing. Acta Pet Et Miner 37(3):445–453 (**in Chinese**)

Tan HB, Ma HZ, Li BK, Zhang XY, Xiao YK (2010) Strontium and boron isotopic constraint on the marine origin of the Khammuane potash deposits in southeastern Laos. Chin Sci Bull 55:3181–3188

Tang DQ, Chen XJ, Zhang XP (2008) Fault systems and their tectonic evolution in XuanHan-DaXian area, the northeastern Sichuan basin. Pet Geol Exp 30(1):58–63 (**in Chinese**)

Wang DS, Zhao YC, Hou DY, Wei XS (1987) Hydrogeochemical feature of subsurface K-rich brine in chuang-25 well and its indication to look for the sylvite minerals. Bull Inst Hydrogeol Eng Geol CAGS 3:41–54 (**in Chinese**)

Wang JS, Xu ZQ, Yu X, Yang Z, Liu W (2011) Discussion of the source of rich potassium element and its precipitation characteristics form green-bean rock. GuangDong Weiliang Yuansu Kexue 18(1):53–58 (**in Chinese**)

Wang CL, Yu XC, Li RQ, Liu LH, Yan K, You C (2021) Origin of lithium-potassium-rich brines in the Jianghan basin, south China: constraints by water-rock reactions of Mesozoic-Cenozoic igneous rocks. Minerals 11(12):1330

Wang FM, Zhong JA, Tang XY, Sheng DB, Liu Z, Pang B (2022) Determination of the bottom boundary of the Middle Triassic Leikoupo formation in the Huangjinkou area of Xuanhan, northeast Sichuan. Geol Bull China 41(2/3):509–515 (**in Chinese**)

Wang KM, Wang ZQ, Zhang YL, Ma SX, Chen L, Xu G (2023) The magmatic constraint for Early Triassic lithium-rich green bean rocks in Sichuan basin and adjacent area. Acta Pet Sin 39(7):2167–2184 (**in Chinese**)

Wen L, Zhang BJ, Chen X, Xu L, Ma HL, Peng HL (2023) Permian and Triassic in Sichuan basin: tectono-sedimentary characteristics and favorable exploration belts. Nat Gas Explor Dev 46(4):1–12 (**in Chinese**)

Xu K, Gong HN (2023) Lithofacies palaeogeographic characteristics and favorable reservoirfacies of the Leikoupo Formation in Sichuan basin. J Palaeogeogr (chinese Edition) 25(4):842–855 (**in Chinese**)

Yan QS (2012) The study of Geological and geochemical characteristics of the brines in Sichuan basin. Ph. D. Dissertation,Chengdu University of Technology, Chengdu, pp 1–117 (in Chinese)

Zhang GW, Guo AL, Dong YP, Yao AP (2019) Rethinking of the Qinling orogen. J Geomech 25(5):746–768 (**in Chinese**)

Zhang B, Liu W, Yang K, Pei WB, Zhang SM, Xiao W (2022) Salt accumulation, potassium formation mechanism and enrichment model of Triassic in northeast Sichuan basin. Earth Sci 47(1):15–26 (**in Chinese**)

Zheng MP, Zhang Z, Zhang YS, Liu XF, Yin HW (2012a) Potash Exploration Characteristics in China: new understanding and research progress. Acta Geosci Sin 33(3):280–294 (**in Chinese**)

Zheng ZJ, Yin HW, Zhang Z, Zheng MP, Yang JX (2012b) Strontium isotope characteristics and the origin of salt deposits in Mengyejing, Yunnan province, SW China. J Nanjing Univ (nat Sci) 48(6):719–727 (**in Chinese**)

Zhong JA, Zheng MP, Tang XY, Liu Z, Liu Z, Wang FM, Cai C, Pang B (2018a) Sedimentary characteristics and genetic study of deep polyhalite in Huangjingkou anticline of northeast Sichuan. Miner Depos 37(1):81–90 (**in Chinese**)

Zhong JA, Zheng MP, Zhang YS, Tang XY, Zhang XF (2018b) The discovery of deep potassium and lithium resources in the Huangjinkou anticline, northeast of Sichuan. Acta Geol Sin 92(03):1279–1280

Zhong JA, Zheng MP, Zhang YS, Tang XY, Zhang XF (2020) Sedimentary and geochemical characteristics of Triassic new type of polyhalite potassium resources in northeast Sichuan and its genetic study. Sci Rep 10(1):13528–13528

Zhou X, Cao Q, Yin F, Guo J, Wang XC, Zhang YS, Wang LD, Sheng Y (2015) Characteristics of the brines and hot springs in the Triassic Carbonatesin the high and steep fold zone of the eastern Sichuan basin. Acta Geol Sin 89(11):1908–1920 (**in Chinese**)

Zhu ZF, Wang GX (1986) Paleogeography of before and after deposition of green-bean rock (altered tuff) between the early and Middle Triassic in the uppper Yangtze platform and its adjacent areas. Oil Gas Geol 7(4):344–355 (**in Chinese**)

Zhu CQ, Qiu NS, Cao HY, Liu YF, Jiang Q (2017) Tectono-thermal evolution of the eastern Sichuan basin:constraints from the vitrinite reflectance and apatite fission track data. Earth Sci Front 24(3):94–104 (**in Chinese**)

Publisher's Note Springer Nature remains neutral with regard to jurisdictional claims in published maps and institutional affiliations.

Springer Nature or its licensor (e.g. a society or other partner) holds exclusive rights to this article under a publishing agreement with the author(s) or other rightsholder(s); author self-archiving of the accepted manuscript version of this article is solely governed by the terms of such publishing agreement and applicable law.